

# Supersymmetry dileptons and trileptons at the Tevatron

JORGE L. LOPEZ<sup>1,2</sup>, D. V. NANOPOULOS<sup>1,2,3</sup>, XU WANG<sup>1,2</sup>, and A. ZICHICHI<sup>4</sup>

<sup>1</sup>*Center for Theoretical Physics, Department of Physics, Texas A&M University  
College Station, TX 77843-4242, USA*

<sup>2</sup>*Astroparticle Physics Group, Houston Advanced Research Center (HARC)  
The Mitchell Campus, The Woodlands, TX 77381, USA*

<sup>3</sup>*CERN Theory Division, 1211 Geneva 23, Switzerland*

<sup>4</sup>*CERN, 1211 Geneva 23, Switzerland*

## Abstract

We consider the production of supersymmetry neutralinos and charginos in  $p\bar{p}$  collisions at the Tevatron, and their subsequent decay via hadronically quiet dileptons and trileptons. We perform our computations in the context of a variety of supergravity models, including generic four-parameter supergravity models, the minimal  $SU(5)$  supergravity model, and  $SU(5) \times U(1)$  supergravity with string inspired two- and one-parameter moduli and dilaton scenarios. Our results are contrasted with estimated experimental sensitivities for dileptons and trileptons for integrated luminosities of  $100 \text{ pb}^{-1}$  and  $1 \text{ fb}^{-1}$ , which should be available in the short and long terms. We find that the dilepton mode is a needed complement to the trilepton signal when the latter is suppressed by small neutralino leptonic branching ratios. The estimated reaches in chargino masses can be as large as 100 (150) GeV for  $100 \text{ pb}^{-1}$  ( $1 \text{ fb}^{-1}$ ). We also discuss the task left for LEP II once the Tevatron has completed its short-term search for dilepton and trilepton production.

Experimental searches for supersymmetric particles have come a long way since the commissioning of the Tevatron  $p\bar{p}$  collider at Fermilab (1988) and the LEP  $e^+e^-$  collider at CERN (1989). The strengths and weaknesses of these two types of colliders are well known. A hadron collider is best suited for searching the highest accessible mass scales since a sharp kinematical limit does not exist, but discoverability depends on the event rate and the cleanliness of the signal. An  $e^+e^-$  collider is capable of discovery essentially up to the kinematical limit, but this is much lower than what would be accessible in a hadron collider. In fact, it has become apparent that an  $e^+e^-$  linear collider with a center-of-mass energy in the multi-hundred GeV range would be ideal for what has been termed “sparticle spectroscopy”. At present though, in the search for new physics we have to make the best possible use of existing facilities, since information gathered there would illuminate the path towards higher energy machines. One such effort is being conducted at the Tevatron, where the search for weakly interacting sparticles (charginos and neutralinos) has become quite topical, in view of the fact that the reach of the machine for the traditional strongly interacting sparticles has been nearly reached. This effort will benefit from an integrated luminosity in excess of  $100\text{ pb}^{-1}$  by the end of the ongoing Run IB, and possibly  $1\text{--}2\text{ fb}^{-1}$  during the Main Injector era around the year 2000.

In this paper we study the prospects for supersymmetry discovery at the Tevatron via the hadronically quiet dilepton and trilepton signals<sup>1</sup> which occur in the production and decay of charginos and neutralinos in  $p\bar{p}$  collisions [1, 2, 3]. Our previous study [3] considered the trilepton signal with an estimated  $100\text{ pb}^{-1}$  of accumulated data. Here we update this analysis by incorporating the latest experimental information on the trilepton signal and prospects for its detection with  $\mathcal{O}(1\text{ fb}^{-1})$  data. We also include for the first time the dilepton signal, which has been recently shown to be experimentally extractable [4], and as we discuss, has the advantage of allowing a significant exploration of the parameter space for chargino masses in the LEP-II accessible range. Our calculations are performed in the context of a broad class of unified supergravity models, which have the virtue of having the least number of free parameters and are therefore highly predictive and straightforwardly testable through a variety of correlated phenomena at different experimental facilities. Our study should give a good idea of the range of possibilities open to experimental investigation, and allow quantitative checks of specific models which yield the largest rates.

We consider unified supergravity models with universal soft supersymmetry breaking at the unification scale, and radiative electroweak symmetry breaking (enforced using the one-loop effective potential) at the weak scale [5]. These constraints reduce the number of parameters needed to describe the models to four, which can be taken to be  $m_{\chi_{1\pm}}, \xi_0 \equiv m_0/m_{1/2}, \xi_A \equiv A/m_{1/2}, \tan\beta$ , with a specified value for the top-quark mass ( $m_t$ ). In what follows we take  $m_t^{\text{pole}} = 160\text{ GeV}$  which is the central value obtained in fits to all electroweak and Tevatron data in the context of supersymmetric models [6]. Of relevance to our discussion, we note that in all models

---

<sup>1</sup>These signals contain no hadronic activity, except for initial state radiation effects, and are thus distinct from the usual multilepton signals in squark and gluino production.

considered the following relation holds to various degrees of approximation

$$m_{\chi_1^\pm} \approx m_{\chi_2^0} \approx 2m_{\chi_1^0} . \quad (1)$$

Among these four-parameter supersymmetric models we consider generic models with continuous values of  $m_{\chi_1^\pm}$  and discrete choices for the other three parameters:

$$\tan\beta = 2, 10 ; \quad \xi_0 = 0, 1, 2, 5 ; \quad \xi_A = 0 . \quad (2)$$

The choices of  $\tan\beta$  are representative; higher values of  $\tan\beta$  are likely to yield values of  $B(b \rightarrow s\gamma)$  in conflict with present experimental limits [7]. The choices of  $\xi_0$  correspond to  $m_{\tilde{q}} \approx (0.8, 0.9, 1.1, 1.9)m_{\tilde{g}}$ . The choice of  $A$  has little impact on the results. We also consider the case of minimal  $SU(5)$  supergravity, where in addition we impose the constraints from proton decay and cosmology (a not too young Universe). The parameter space in this case is still four-dimensional, but restricted to  $\tan\beta \lesssim 10$ ,  $\xi_0 \gtrsim 4$ , and  $m_{\chi_1^\pm} \lesssim 120$  GeV [8].

We also consider the case of no-scale  $SU(5) \times U(1)$  supergravity [5]. In this class of models the supersymmetry breaking parameters are related in a string-inspired way. In the two-parameter *moduli* scenario  $\xi_0 = \xi_A = 0$  [9], whereas in the *dilaton* scenario  $\xi_0 = \frac{1}{\sqrt{3}}$ ,  $\xi_A = -1$  [10]. We also compute the rates in the *one-parameter* moduli ( $B(M_U) = 0$ ) and dilaton ( $B(M_U) = 2m_0$ ) scenarios, where  $M_U$  is the string unification scale, and with this extra condition  $\tan\beta$  is determined as a function of  $m_{\chi_1^\pm}$ , which is the only free parameter in the model. A series of experimental constraints and predictions for these models have been given in Refs. [11] and [12], respectively.

The processes of interest are

- *Trileptons*:  $p\bar{p} \rightarrow \chi_2^0\chi_1^\pm$ , where the next-to-lightest neutralino decays leptonically ( $\chi_2^0 \rightarrow \chi_1^0\ell^+\ell^-$ ), and so does the lightest chargino ( $\chi_1^\pm \rightarrow \chi_1^0\ell^\pm\nu_\ell$ ). The cross section proceeds via  $s$ -channel exchange of an off-shell  $W$  and (small)  $t$ -channel squark exchange, and thus peaks at  $m_{\chi_1^\pm} \approx \frac{1}{2}M_W$ , and otherwise falls off smoothly with increasing chargino masses with a small  $\tan\beta$  dependence.
- *Dileptons*:  $p\bar{p} \rightarrow \chi_1^+\chi_1^-$ , where both charginos decay leptonically. The cross section proceeds via  $s$ -channel exchange of off-shell  $Z$  and  $\gamma$  and  $t$ -channel squark exchange, and peaks for  $m_{\chi_1^\pm} \approx \frac{1}{2}M_Z$ . Dileptons could also come from  $p\bar{p} \rightarrow \chi_1^0\chi_2^0, \chi_2^0\chi_2^0$ , with the appropriate leptonic or invisible decays of  $\chi_2^0$ . Both of these processes are negligible [2] because the couplings of the  $Z$  and  $\gamma$  to neutralinos are highly suppressed when the neutralinos have a high gaugino content, as is the case when Eq. (1) holds. Yet another source of dileptons via  $p\bar{p} \rightarrow \tilde{e}_R^+\tilde{e}_R^-$  suffers from small rates for selectron masses beyond the LEP limit [13].

The more important factors in the dilepton and trilepton yields are the leptonic branching fractions which can vary widely throughout the parameter space [3]. If all sparticles are fairly heavy, the decay amplitude is dominated by  $W$  or  $Z$  exchange. In this case the branching fractions into electrons plus muons are  $B(\chi_1^\pm \rightarrow \chi_1^0 \ell^\pm \nu_l) \approx 2/9$  and  $B(\chi_2^0 \rightarrow \chi_1^0 \ell^+ \ell^-) \approx 6\%$ . On the other hand, if some of the sparticles are relatively light, most likely the sleptons, the branching fractions are altered. The extreme, although not unusual, case occurs when the sleptons are on-shell. These two-body decays then dominate and the chargino leptonic branching fraction is maximized, *i.e.*,  $B(\chi_1^\pm \rightarrow \chi_1^0 \ell^\pm \nu_l)_{\max} = 2/3$ . Light sleptons also affect the neutralino leptonic branching ratio.<sup>2</sup> When the sneutrino is on-shell and is lighter than the corresponding right-handed charged slepton ( $\tilde{e}_R, \tilde{\mu}_R$ ), the channel  $\chi_2^0 \rightarrow \nu_l \tilde{\nu}_l$  dominates the amplitude, and the neutralino leptonic branching ratio is suppressed. This situation is reversed when the charged slepton is on-shell and is lighter than the sneutrino, which leads to an enhancement of the neutralino leptonic branching ratio. For sufficiently high neutralino and chargino masses, both leptonic branching ratios decrease because the  $W$  and  $Z$  go on-shell and dominate the decay amplitudes. In the case of the neutralino, the spoiler mode  $\chi_2^0 \rightarrow \chi_1^0 h$  also becomes kinematically allowed. These high-mass suppressions do not kick in until chargino and neutralino masses  $m_{\chi_1^\pm} \approx m_{\chi_2^0} \sim 2M_Z, 2m_h \sim 200$  GeV.

The results of our computations for the various models are shown in Figs. 1,2, 3,4,5,6. The various curves in the figures terminate at the low end because of various parameter space constraints, whereas at the high end they are cutoff when the yields fall below the foreseeable sensitivity.<sup>3</sup> In most cases we note that the rates are higher for  $\mu < 0$ . This is a consequence of suppressed branching fractions for  $\mu > 0$ , but also a generally smaller allowed parameter space which requires minimum values of the chargino mass which may exceed significantly the present experimental lower limit. We can also observe that the dilepton rates indeed peak near  $\frac{1}{2}M_Z$ , whereas the trilepton rates are not as large for light chargino masses since they peak at  $\frac{1}{2}M_W$ . It is also evident in the figures that for chargino masses below  $\sim 100$  GeV, the trilepton rates can be highly suppressed, while the dilepton rates are not, thus producing a rather complementary effect. This “threshold” phenomenon is most evident in Figs. 4,5,6 and, as discussed above, corresponds to a suppression of the neutralino leptonic branching ratio for light sleptons, *i.e.*, when  $\chi_2^0 \rightarrow \nu \tilde{\nu}$  is allowed.

The significance of our results is quantified by the horizontal dashed lines in the figures, which represent estimates of the experimental sensitivity to be reached with  $100 \text{ pb}^{-1}$  (upper lines) and  $1 \text{ fb}^{-1}$  (lower lines). The lesser sensitivity should be achievable at the end of Run IB during 1995 (*i.e.*, prior to the LEP II upgrade), whereas the higher sensitivity should be available with the Main Injector upgrade in 1999 (*i.e.*, after the LEP II shutdown but before the LHC commissioning).

The trilepton sensitivity with  $100 \text{ pb}^{-1}$  (*i.e.*,  $0.4 \text{ pb}$ ) has been estimated by

---

<sup>2</sup>In supergravity models  $m_{\tilde{e}_R} = m_{\tilde{\mu}_R} < m_{\tilde{e}_L} = m_{\tilde{\mu}_L}$ .

<sup>3</sup>For  $\xi_0 = 5$ , radiative electroweak symmetry breaking is only possible for  $\tan \beta \lesssim 4$ . This is why there is no curve for  $\xi_0 = 5$  in Fig. 2 ( $\tan \beta = 10$ ), whereas there is such a curve in Fig. 1 ( $\tan \beta = 2$ ).

Table 1: Estimated chargino mass reaches in various supergravity models for chargino-neutralino production in  $p\bar{p}$  collisions at the Tevatron via dilepton and trilepton modes for integrated luminosities of  $100 \text{ pb}^{-1}$  and  $1 \text{ fb}^{-1}$ . All masses in GeV. Dashes (-) indicate negligible sensitivity.

generic		$\mu > 0$		$\mu < 0$	
$\tan \beta$	$\xi_0$	$100 \text{ pb}^{-1}$	$1 \text{ fb}^{-1}$	$100 \text{ pb}^{-1}$	$1 \text{ fb}^{-1}$
2	0	-	120	100	145
	1	-	125	75	115
	2	-	100	65	100
	5	-	80	55	80
10	0	-	105	70	135
	1	70	95	65	100
	2	-	70	-	70

Model		$\mu > 0$		$\mu < 0$	
	$\tan \beta$	$100 \text{ pb}^{-1}$	$1 \text{ fb}^{-1}$	$100 \text{ pb}^{-1}$	$1 \text{ fb}^{-1}$
moduli (2-par)	2	-	115	100	150
	6	75	160	100	150
	10	75	160	70	150
dilaton (2-par)	2	95	135	80	120
	6	80	130	80	120
	10	80	125	80	120
moduli (1-par)		N/A	N/A	70	150
dilaton (1-par)		N/A	N/A	80	125
minimal $SU(5)$		50	80	50	75

simply scaling down by a factor of 5 the present experimental limit of  $\sim 2 \text{ pb}$  obtained with  $20 \text{ pb}^{-1}$  of recorded data [14]. The factor of 5 is the expected increase in recorded luminosity, and a simple  $\mathcal{L}$  scaling is appropriate assuming the trilepton signal has no Standard Model backgrounds at this level of sensitivity. The sensitivity at  $1 \text{ fb}^{-1}$  requires a study of the background since small Standard Model processes and detector-dependent instrumental backgrounds become important at this level of sensitivity [15]. The sensitivity in the figures (*i.e.*,  $0.07 \text{ pb}$ ) is obtained by scaling up by  $\sqrt{\mathcal{L}}$  the value given in Table II of Ref. [15].

The dilepton (plus  $\cancel{p}_T$ ) signal suffers from several Standard Model backgrounds, most notably  $Z \rightarrow \tau\tau$  and  $WW$  production. A study based on the D0 detector [4] reveals that with suitable cuts, in  $100 \text{ pb}^{-1}$  an estimated background of 8 events is expected, which would require 8 signal events at  $3\sigma$  significance. The efficiencies for dilepton detection have also been studied [4], and they improve with increasing chargino masses, 8% is a typical value. All this implies a sensitivity of 1 pb for

dilepton detection. With  $1 \text{ fb}^{-1}$  one can scale down the sensitivity with  $\sqrt{\mathcal{L}}$ , obtaining a sensitivity of 0.3 pb.

The reaches in chargino masses in the various models, can be readily obtained from the figures by considering both dilepton and trilepton signals, and are summarized in Table 1 for the two integrated luminosity scenarios. The reaches in Table 1 translate into indirect reaches in every other sparticle mass, since they are all related. In particular,  $m_{\chi_1^\pm} \sim 0.3m_{\tilde{g}}$  and  $m_{\tilde{q}} \approx (m_{\tilde{g}}/2.9)\sqrt{6 + \xi_0^2}$  (in the  $SU(5) \times U(1)$  models the numerical coefficients in this relation are slightly different, implying  $m_{\tilde{q}} \approx m_{\tilde{g}}$ ). It is also interesting to point out that the pattern of yields for the various models is quite different, therefore observation of a signal will disprove many of the models, while supporting a small subset of them.

It has been pointed out that the dilepton and trilepton data sample may be enhanced by considering presumed trilepton events where one of the leptons is either missed or has a  $p_T$  below 5 GeV (“2-out-of-3”) [16]. Such enhancements would alter our reach estimates above, making them even more promising.

From Table 1 it is clear that in some regions of parameter space, the reach of the Tevatron for chargino masses is quite significant. With  $100 \text{ pb}^{-1}$  it should be possible to probe chargino masses as high as 100 GeV in the generic models for  $\tan\beta = 2$ ,  $\xi_0 = 0$ , and  $\mu < 0$ , and in the two-parameter  $SU(5) \times U(1)$  moduli scenario for  $\tan\beta \lesssim 10$ . More generally, the accessible region of parameter space should overlap with that within the reach of LEP II, although it would have been explored before LEP II turns on. However, LEP II has an important task: chargino searches at LEP II will not be hindered by small branching fractions, and thus a more model-independent lower limit on the chargino mass should be achievable, *i.e.*,  $m_{\chi_1^\pm} \lesssim \frac{1}{2}\sqrt{s}$ .<sup>4</sup> We would like to conclude with Fig. 6, where we show the predictions for the dilepton and trilepton rates in our chosen one-parameter  $SU(5) \times U(1)$  models, which are the most predictive supersymmetric models to date. It is interesting to note that in the moduli scenario, the mass reach for charginos could be as high as 150 GeV with an integrated luminosity of  $1 \text{ fb}^{-1}$ . Further proposed increases in luminosity or center-of-mass energy of the Tevatron collider have the potential of probing even deeper into the parameter space [15]. We conclude that detection of weakly interacting sparticles at the Tevatron may well bring the first direct signal for supersymmetry.

## Acknowledgments

We would like to thank James White for motivating this study and for providing us with valuable information about the sensitivity of the dilepton signal. This work has been supported in part by DOE grant DE-FG05-91-ER-40633. The work of X. W. has been supported by the World Laboratory.

---

<sup>4</sup>At LEP II it might be possible to extend the indirect reach for charginos by studying the process  $e^+e^- \rightarrow \chi_1^0\chi_2^0$  with  $\chi_2^0 \rightarrow \chi_1^0 + 2j$ . Equation (1) implies a kinematical reach of  $m_{\chi_1^\pm} \lesssim \frac{2}{3}\sqrt{s}$ .

## References

- [1] J. Ellis, J. Hagelin, D. V. Nanopoulos, and M. Srednicki, Phys. Lett. B **127** (1983) 233; P. Nath and R. Arnowitt, Mod. Phys. Lett. A **2** (1987) 331; R. Barbieri, F. Caravaglios, M. Frigeni, and M. Mangano, Nucl. Phys. B **367** (1991) 28.
- [2] H. Baer and X. Tata, Phys. Rev. D **47** (1993) 2739; H. Baer, C. Kao, and X. Tata, Phys. Rev. D **48** (1993) 5175.
- [3] J. L. Lopez, D. V. Nanopoulos, X. Wang, and A. Zichichi, Phys. Rev. D **48** (1993) 2062.
- [4] J. White and D. Norman, D0 Note 2395.
- [5] For a recent review see *e.g.*, J. L. Lopez, D. V. Nanopoulos, and A. Zichichi, Prog. Part. Nucl. Phys. **33** (1994) 303.
- [6] J. Ellis, G.L. Fogli and E. Lisi, Phys. Lett. B **333** (1994) 118; J. Erler and P. Langacker, UPR-0632T (hep-ph/9411203).
- [7] J. L. Lopez, D. V. Nanopoulos, X. Wang, and A. Zichichi, Phys. Rev. D **51** (1995) 147.
- [8] J. L. Lopez, D. V. Nanopoulos, and H. Pois, Phys. Rev. D **47** (1993) 2468; J. L. Lopez, D. V. Nanopoulos, H. Pois, and A. Zichichi, Phys. Lett. B **299** (1993) 262; J. L. Lopez, D. V. Nanopoulos, and K. Yuan, Phys. Rev. D **48** (1993) 2766.
- [9] J. L. Lopez, D. V. Nanopoulos, and A. Zichichi, Phys. Rev. D **49** (1994) 343.
- [10] J. L. Lopez, D. V. Nanopoulos, and A. Zichichi, Phys. Lett. B **319** (1993) 451.
- [11] J. L. Lopez, D. V. Nanopoulos, G. Park, X. Wang, and A. Zichichi, Phys. Rev. D **50** (1994) 2164.
- [12] J. L. Lopez, D. V. Nanopoulos, and A. Zichichi, Texas A & M University preprint CTP-TAMU-27/94 (hep-ph/9408345).
- [13] H. Baer, C. Chen, F. Paige, and X. Tata, Phys. Rev. D **49** (1994) 3283.
- [14] CDF Collaboration, Y. Kato, in “Proceedings of the 9th Topical Workshop on Proton-Antiproton Collider Physics,” Tsukuba, Japan, October 1993, edited by K. Kondo and S. Kim (Universal Academy Press, Tokyo), p. 291; CDF Collaboration, Fermilab-Conf-94/149-E (1994), to appear in Proceedings of the 27th International Conference on High Energy Physics, Glasgow, July 20–27, 1994.
- [15] T. Kamon, J. L. Lopez, P. McIntyre, and J. White, Phys. Rev. D **50** (1994) 5676.
- [16] J. White, private communication.

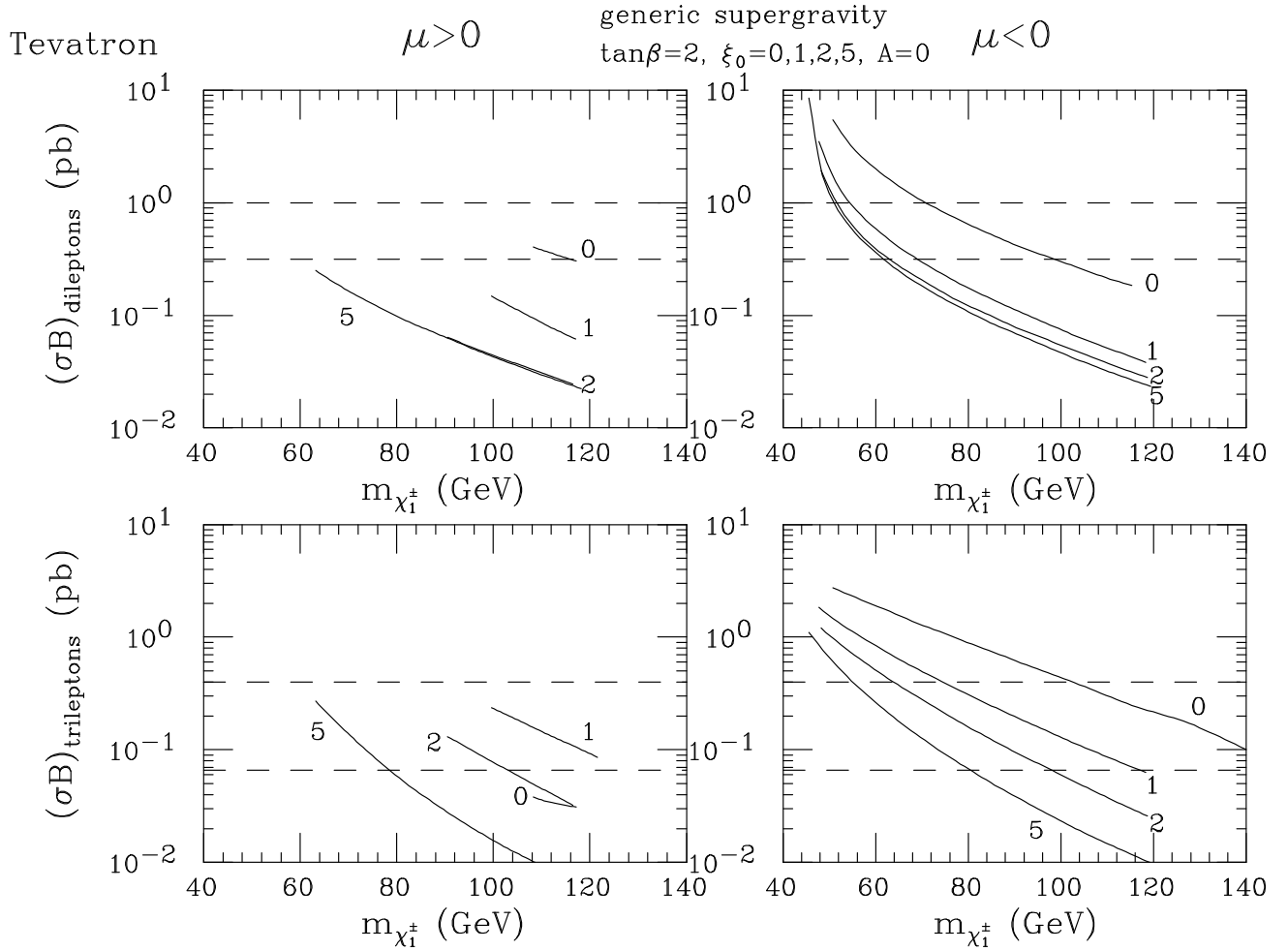


Figure 1: The dilepton and trilepton rates at the Tevatron versus the chargino mass in a generic unified supergravity model with  $\tan\beta = 2$ ,  $\xi_0 = 0, 1, 2, 5$  (as indicated), and  $A = 0$ . The upper (lower) dashed lines represent estimated reaches with  $100 \text{ pb}^{-1}$  ( $1 \text{ fb}^{-1}$ ) of data.



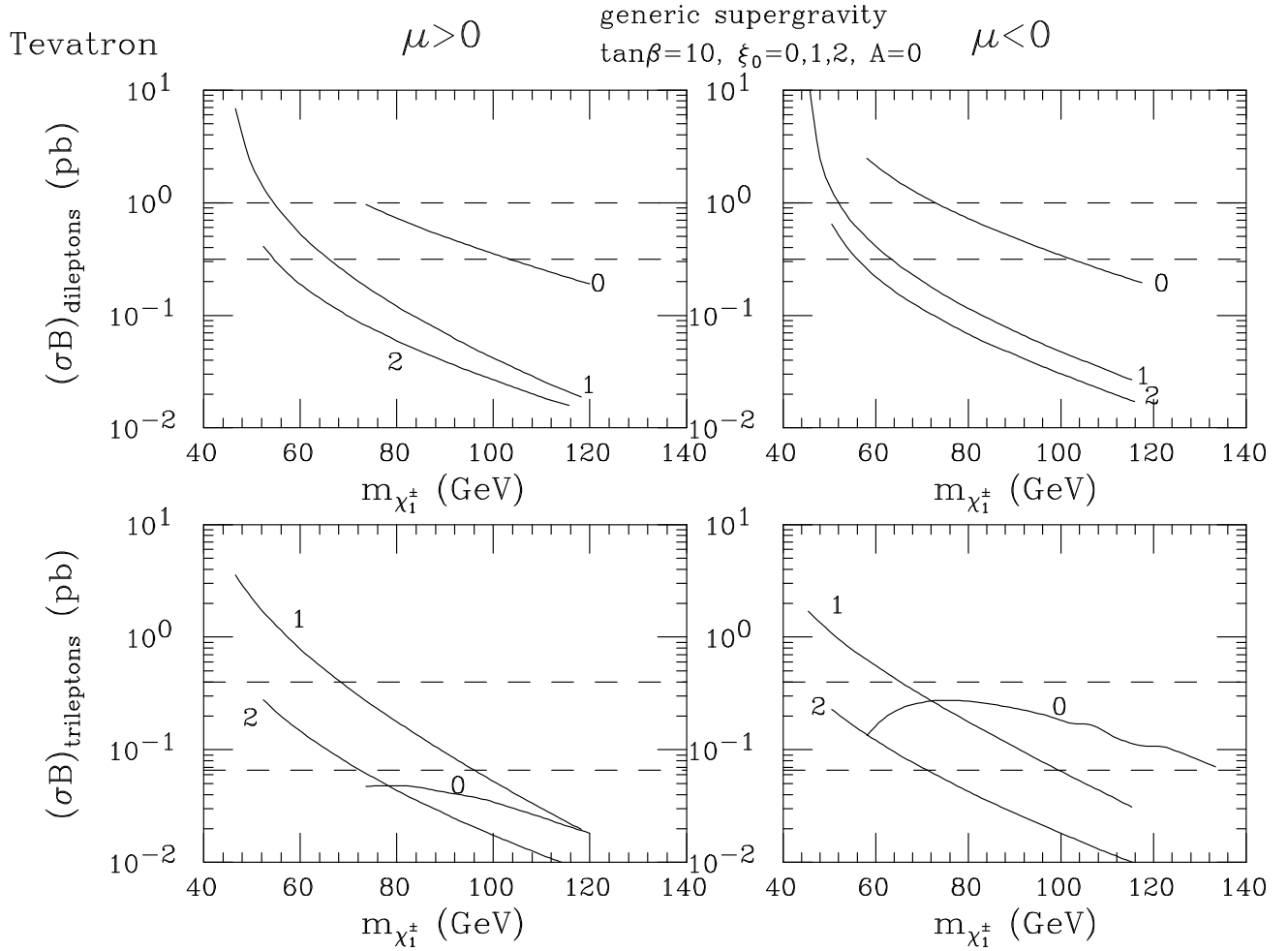


Figure 2: The dilepton and trilepton rates at the Tevatron versus the chargino mass in a generic unified supergravity model with  $\tan\beta = 10$ ,  $\xi_0 = 0, 1, 2$  (as indicated), and  $A = 0$ . The upper (lower) dashed lines represent estimated reaches with  $100 \text{ pb}^{-1}$  ( $1 \text{ fb}^{-1}$ ) of data.

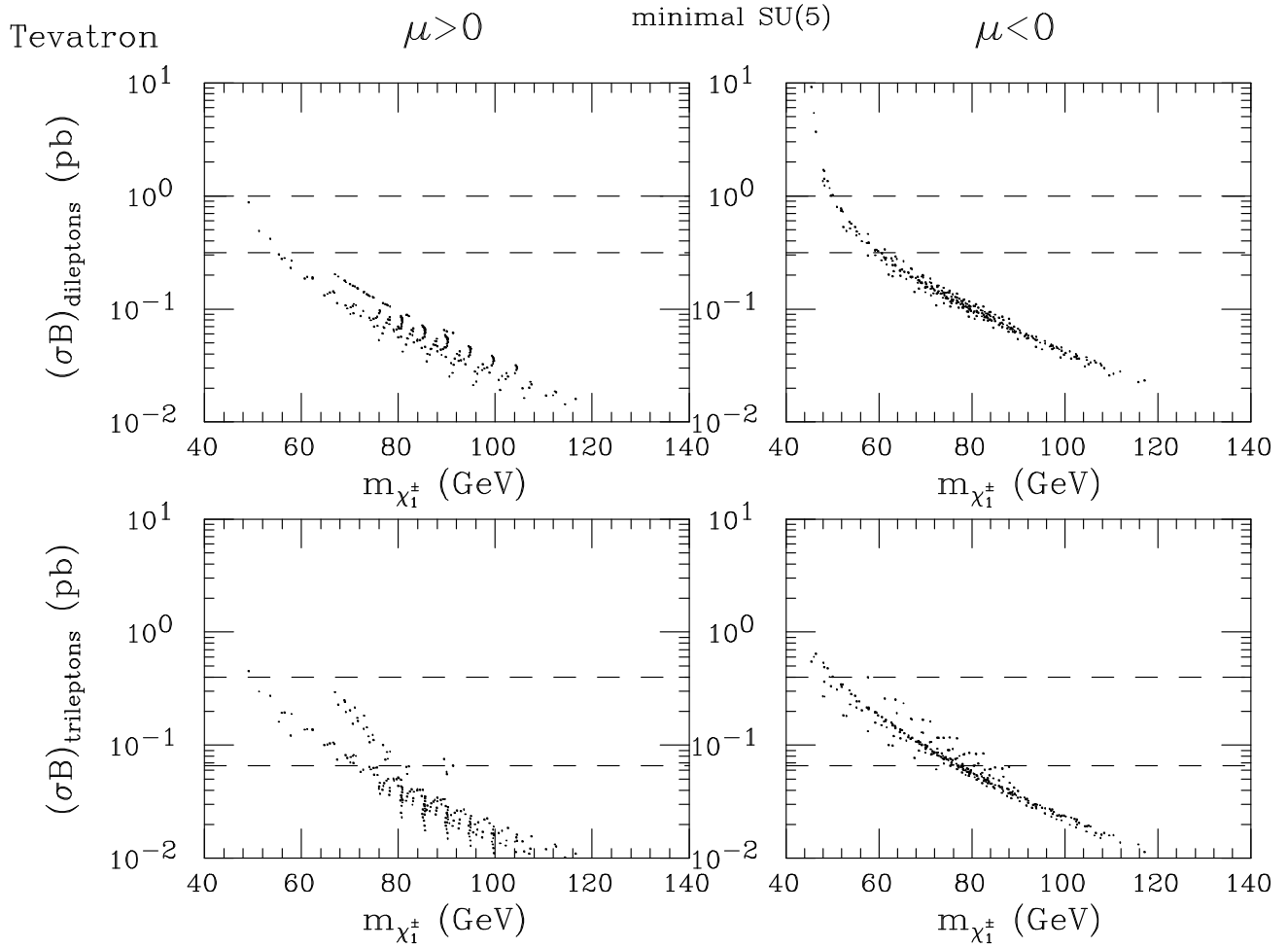


Figure 3: The dilepton and trilepton rates at the Tevatron versus the chargino mass in the minimal  $SU(5)$  supergravity model (where  $\tan\beta < 10$ ,  $\xi_0 > 4$ ). The upper (lower) dashed lines represent estimated reaches with  $100 \text{ pb}^{-1}$  ( $1 \text{ fb}^{-1}$ ) of data.

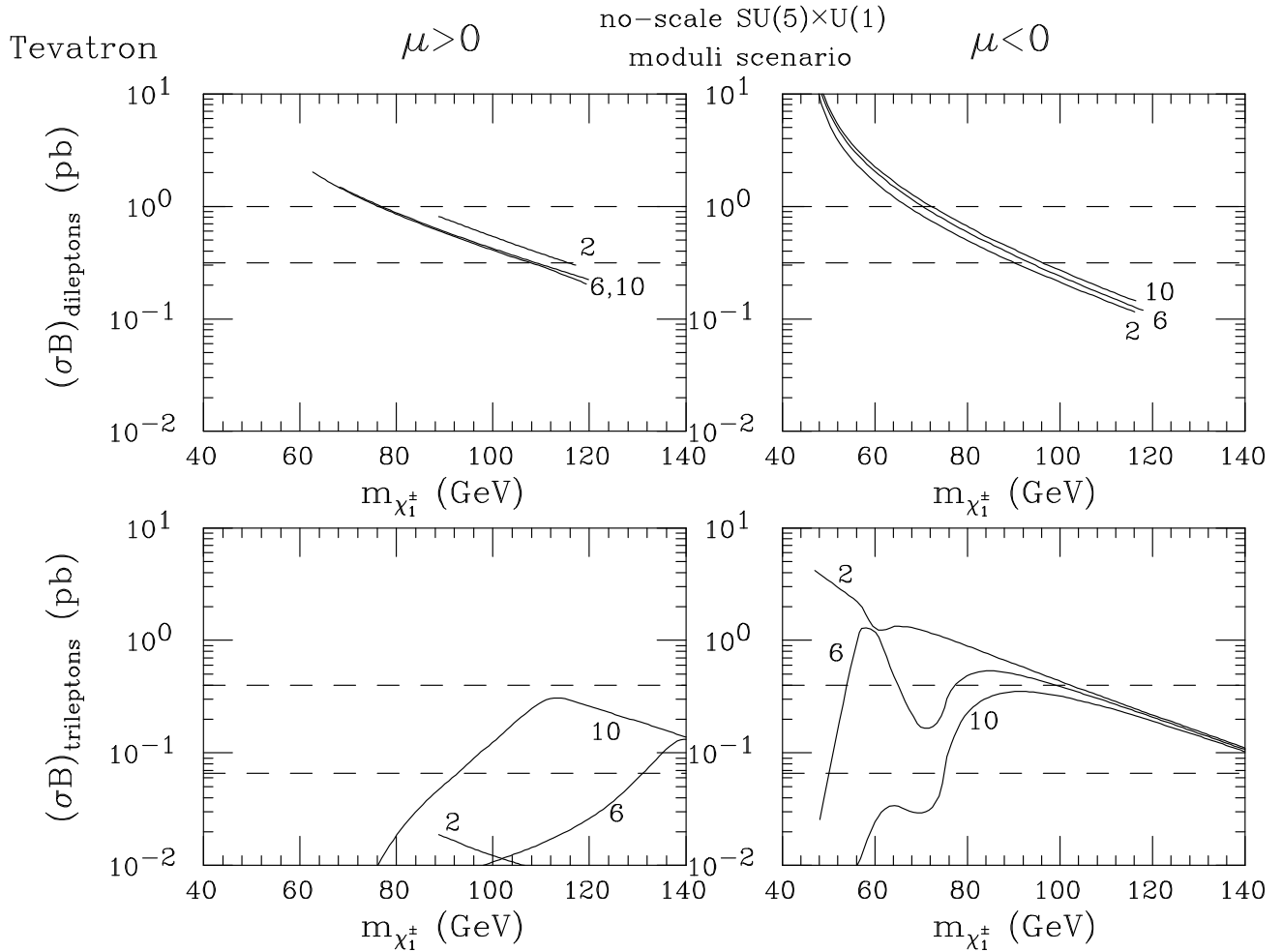


Figure 4: The dilepton and trilepton rates at the Tevatron versus the chargino mass in two-parameter  $SU(5) \times U(1)$  supergravity – moduli scenario ( $\xi_0 = \xi_A = 0$ ) for the indicated values of  $\tan \beta$ . The upper (lower) dashed lines represent estimated reaches with  $100 \text{ pb}^{-1}$  ( $1 \text{ fb}^{-1}$ ) of data.

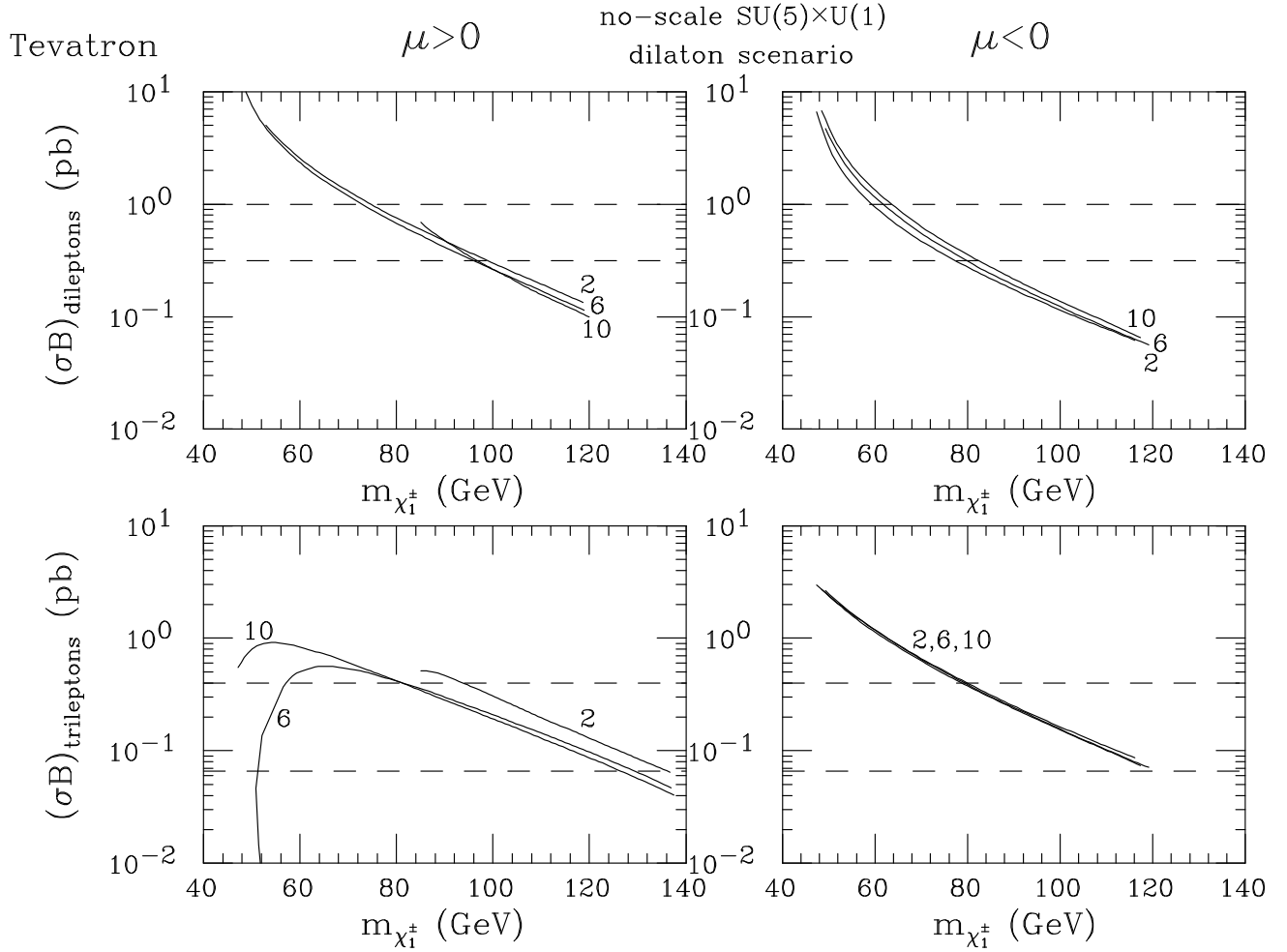


Figure 5: The dilepton and trilepton rates at the Tevatron versus the chargino mass in two-parameter  $SU(5) \times U(1)$  supergravity – dilaton scenario ( $\xi_0 = \frac{1}{\sqrt{3}}, \xi_A = -1$ ) for the indicated values of  $\tan\beta$ . The upper (lower) dashed lines represent estimated reaches with  $100\text{pb}^{-1}$  ( $1\text{fb}^{-1}$ ) of data.

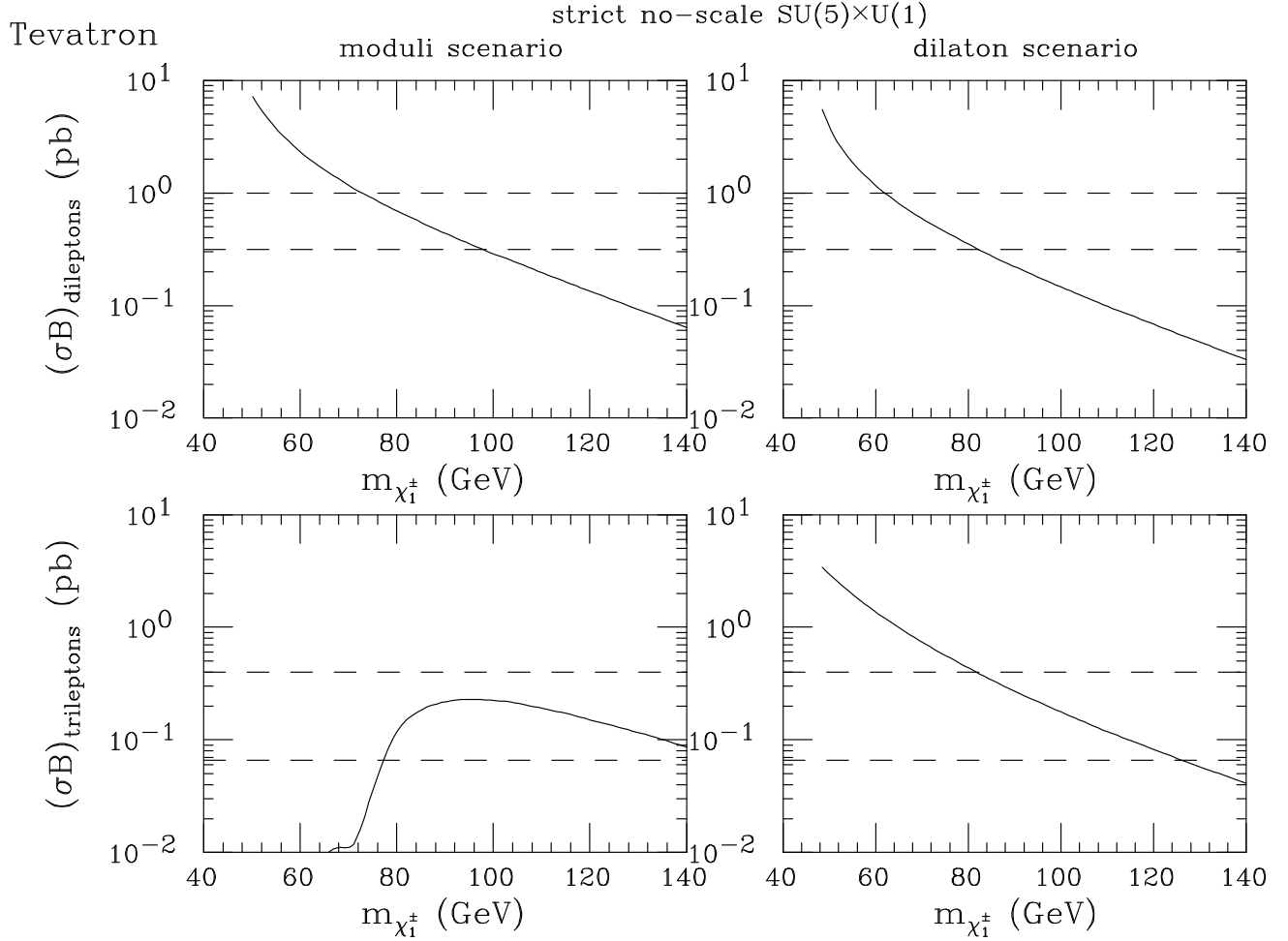


Figure 6: The dilepton and trilepton rates at the Tevatron versus the chargino mass in one-parameter  $SU(5) \times U(1)$  supergravity – moduli and dilaton scenarios ( $\mu < 0$  in both cases). The upper (lower) dashed lines represent estimated reaches with  $100 \text{ pb}^{-1}$  ( $1 \text{ fb}^{-1}$ ) of data.

This figure "fig1-1.png" is available in "png" format from:

<http://arxiv.org/ps/hep-ph/9412346v1>

This figure "fig1-2.png" is available in "png" format from:

<http://arxiv.org/ps/hep-ph/9412346v1>

This figure "fig1-3.png" is available in "png" format from:

<http://arxiv.org/ps/hep-ph/9412346v1>



This figure "fig1-4.png" is available in "png" format from:

<http://arxiv.org/ps/hep-ph/9412346v1>

This figure "fig1-5.png" is available in "png" format from:

<http://arxiv.org/ps/hep-ph/9412346v1>

This figure "fig1-6.png" is available in "png" format from:

<http://arxiv.org/ps/hep-ph/9412346v1>